Compound nuclear evaporation model calculations in the mass $A \sim 50$ and $A \sim 80$ regions

L. V. Theisen,* L. R. Medsker,† and S. L. Tabor
Department of Physics, Florida State University, Tallahassee, Florida 32306
(Received 20 December 1982)

Experimental excitation functions for the products of the reactions ^{27}Al + ^{28}Si, ^{28}Si + ^{28}Si, ^{54}Fe + ^{28}Si, and ^{56}Fe + ^{28}Si were measured over the energy range from 65 to 99 MeV. The experimental excitation functions of the reaction products were then compared to the results obtained from compound nuclear evaporation model calculations. The generally better agreement obtained with one of the codes suggests the importance of angular momentum effects in the exit channel. Two-particle evaporations are badly underpredicted by both calculations in both mass regions. It is possible that part of these cross sections result from some reaction mechanism other than compound nuclear. The compound nuclear evaporation model calculations are also very sensitive to the level density parameters a, which are not well known in the mass $A \sim 50$ and $A \sim 80$ regions.

[NUCLEAR REACTIONS ^{27}Al(^{28}Si,$xpyn\gamma$) and ^{28}Si(^{28}Si,$xpyn\gamma$) $E_{lab}=65-90$ MeV; measured $\sigma(E_\gamma,E)$. ^{54}Fe(^{28}Si,$xpyn\gamma$) and ^{56}Fe(^{28}Si,$xpyn\gamma$) $E_{lab}=80-99$ MeV; measured $\sigma(E_\gamma,E)$. Enriched targets.]

I. INTRODUCTION

This work is part of a continuing program at Florida State University utilizing ^{28}Si beams along with in-beam γ-ray spectroscopy to study heavy-ion-induced fusion reactions in the mass $A \sim 50$ and $A \sim 80$ regions. Few statistical model calculations have previously been done in the mass $A \sim 80$ region.[1–4] In the following we attempt to bridge the gap between a mass region ($A \sim 50$) where statistical model calculations have been previously done and one ($A \sim 80$) in which few studies have been made. A comparison of experimental evaporation residue cross sections with those from statistical model calculations was made for the reaction products produced with the reactions ^{27}Al+^{28}Si, ^{28}Si+^{28}Si, ^{54}Fe+^{28}Si, and ^{56}Fe+^{28}Si. In this way, the usefulness of these calculations for predicting evaporation residue cross sections can be determined. The results of in-beam γ-ray spectroscopy experiments with these reactions have been reported previously in Refs. 5–8.

Two computer programs ALICE (Ref. 9) and LILITA (Ref. 10) based on two different theoretical calculations were used for this study. ALICE uses the Weisskopf-Ewing[11,12] formalism and LILITA uses the Hauser-Feshbach[13] formalism to calculate evaporation residue cross sections for multiple particle emissions. The major difference between these calculations is that ALICE ignores angular momentum effects in the exit channels, while LILITA includes these effects. In fact, if conservation of angular momentum were removed from the Hauser-Feshbach (i.e., LILITA) approach it would reduce to the Weisskopf-Ewing (i.e., ALICE) approach. Because angular momentum effects in the exit channels are included in LILITA, the number of exit channels becomes quite large and the calculation becomes very complicated. That is, each allowed evaporation channel is now multiplied by the allowed values of angular momentum, thus greatly increasing the number of possible exit channels. The LILITA calculations are made possible by the use of Monte Carlo techniques.

II. EXPERIMENTAL PROCEDURE

An inverted sputter ion source[14] was used to produce beams of ^{28}Si which were injected into the Florida State University Super *FN* Tandem Van de Graaff accelerator. ^{28}Si beams with energies of 65 to 99 MeV and currents of 10 to 30 nA on target were used. Experiments were carried out using targets of ^{27}Al, ^{28}Si, ^{54}Fe, and ^{56}Fe evaporated onto tantalum backings 0.53 mm thick. Target thicknesses were 350 μg/cm^2 for ^{27}Al, 400 μg/cm^2 for ^{28}Si, 100 μg/cm^2 for ^{54}Fe, and 400 μg/cm^2 for ^{56}Fe.

Gamma rays from the different reaction products produced with the reactions $^{27}Al+^{28}Si$, $^{28}Si+^{28}Si$, $^{54}Fe+^{28}Si$, and $^{56}Fe+^{28}Si$ were detected with a Ge(Li) detector. This detector has an 18.6% efficiency at 25 cm source-to-detector distance, relative to a 7.6×7.6 cm NaI(Tl) detector. The energy resolution was 2.0 keV full width at half maximum (FWHM) at 1.33 MeV. Efficiency and energy calibrations were obtained using a National Bureau of Standards[15] (NBS) mixed radionuclide source, which produces γ rays of known energy and intensities. The source was placed at the target location inside the scattering chamber for calibration. Checks of the energy calibrations were also obtained using γ rays produced with the contaminant reactions $^{16}O+^{28}Si$ and $^{12}C+^{28}Si$.

Excitation functions—measurements of intensity as a function of beam energy—were taken in 5 MeV steps over the laboratory energy ranges of 65–80 MeV for $^{27}Al+^{28}Si$, 65–90 MeV for $^{28}Si+^{28}Si$, and 80–99 MeV for $^{54}Fe+^{28}Si$ and $^{56}Fe+^{28}Si$. The step size is acceptable because we are only interested in the overall shapes and not the fine structure of the excitation functions. Furthermore, the energy loss in the targets was on the order of 3 MeV. Normalization between beam energies was obtained by using the total integrated beam charge. The singles γ-ray spectra for the excitation functions were measured at an angle of 90° to the beam axis. These measurements were used to obtain accurate values for the relative intensities of γ rays. The singles spectra were analyzed using a modified version of the computer code PEAKFIT.[16] The program performs a least squares fit of Gaussian distributions to the peaks in a spectrum by varying the FWHM, height, and background parameters of the Gaussian curves in an iterative procedure to best agree with the data.

Intensity measurements of the γ rays originating from all transitions to the ground state of a residual nucleus were used for relative cross section measurements. These transitions were summed to form the evaporation residue relative cross section for a given residual nucleus. The heavy-ion reactions used produced highly aligned residual nuclei which decay primarily down the yrast line to the ground state. Therefore, the transitions mentioned above are believed to be representative of the cross sections of the respective residual nuclei. Also, the direct population of the ground states of residual nuclei from these reactions is expected to be small, because of the high energies and large angular momenta involved.

In practice, calculations used for γ-ray spectroscopy only need relative cross sections for use in predicting product yields. Therefore, relative instead of absolute cross sections of the residual nuclei were measured. In addition, LILITA (Ref. 10) does not calculate absolute cross sections, but, rather, relative cross sections, due to the complexity of the calculation.

Corrections to the ground state transitions were made for the anisotropy of the γ-ray intensities and for feeding due to radioactivities produced in the target. The intensity corrected for the anisotropy of the γ emission is $I_0=I(\theta)/W(\theta)$, where $I(\theta)$ is the intensity of the γ ray at an angle θ, and $W(\theta)$ is obtained from fitting angular distribution data for the γ-ray transition to a Legendre polynomial function.

The angular distribution measurements were made only at one energy. The correction obtained at this energy for the anistropy of the γ-ray intensity was then used for all energies, since the angular distributions are expected to be similar over the energy range of interest.[17–19]

The correction for feeding due to radioactivities was obtained by using the equation $I_d=I_p(1-e^{\lambda t})P$. I_d is the intensity of the daughter nucleus (the nucleus for which the correction is needed) due to feeding from the parent nucleus, and I_p is the measured intensity of the parent nucleus. P is the fraction of the time the parent feeds that level in the daughter nucleus whose ground state transition is being studied. λ equals $0.693/T_{1/2}$, where $T_{1/2}$ is the half-life of the parent nucleus. Finally, t is the amount of time for which the data were collected. After all corrections to the intensities were made, the resulting cross sections were compared to those obtained from statistical model calculations. The errors in the experimental evaporation residue cross sections were from 10 to 20%.

III. DISCUSSION OF CALCULATIONS

Many heavy-ion reactions are well described by the fusion or compound nucleus reaction process. In these reactions large numbers of compound states are excited and the phases between these states are distributed randomly, so the decay of the compound nucleus is independent of its formation.[20] As stated above, two statistical model calculations were used for this study: (1) ALICE, which uses a standard Weisskopf-Ewing evaporation calculation with multiple particle emission of n, p, d, and α particles, and (2) LILITA, which uses a Hauser-Feshbach calculation in conjunction with the Monte-Carlo method to predict the relative intensities of reaction products.

A. ALICE

The computer code ALICE (Ref. 9) evaluates the Weisskopf-Ewing[11,12] formula over a weighted distribution of emitting nucleus excitation energies for

all but the first particle emitted. This is done in 1 MeV intervals for the emission of n, p, d, and α particles. The default options for this code were used in our calculations. An optical model routine contained in ALICE was used to calculate the particle emission probabilities. The rigid body moment of inertia was used in the ALICE calculations. The S-wave calculation option was not used. The level densities in the daughter nuclei were calculated using a Fermi gas level density without a pairing energy correction. A value of $A/8$ was chosen for the level density parameter because it approximately reproduces the experimental results over a large region of nuclei.[21]

B. LILITA

The second computer code used for the calculation of evaporation residue cross sections was LILITA.[10] LILITA is a Hauser-Feshbach[13] calculation allowing for multiple particle emissions and is used in conjunction with the Monte Carlo method.

In the Hauser-Feshbach picture, the compound nucleus statistically decays into all possible channels, where the number of available channels changes rapidly with the angular momentum of the compound nucleus. The Hauser-Feshbach[13] formula is

$$\sigma(\alpha,\alpha')=\pi\lambda\hat{}^2\sum\frac{(2J+1)}{(2I+1)(2i+1)}\frac{\sum_{l's'}T^J_{\alpha'l's'}\sum_{ls}T^J_{\alpha ls}}{\sum_{\alpha''l''s''}T^J_{\alpha''l''s''}},$$

where α,l,s refer to the incident channel, α',l',s' to the exit channel, and α'',l'',s'' to all possible channels. Each channel α has channel spin s, orbital angular momentum l, and total angular momentum J; and i and I are the intrinsic spins of the projectile and target nucleus, respectively. The summation in the denominator is over all known discrete levels and continuum levels computed from level density equations.[13]

The fusion cross section for the compound nucleus is

$$\sigma_{\rm fus}=\pi\lambda\hat{}^2\sum\frac{2J+1}{(2I+1)(2i+1)}\sum T^J_{\alpha ls},$$

where $T^J_{\alpha ls}$ are the optical model transmission coefficients describing the probability of compound nucleus formation in state α. If the sharp-cutoff model is used for the transmission coefficients, the fusion cross section reduces to

$$\sigma_{\rm fus}=\pi\lambda\hat{}^2(J_c+1)^2,$$

where J_c is defined as the critical angular momentum, (i.e., $T^J_{\alpha ls}=1$ for $J\le J_c$ and $T^J_{\alpha ls}=0$ for $J>J_c$).[22] This leads to the determination of the compound nucleus momentum probability density function

$$P_J=\frac{(2J+1)}{(J_c+1)^2}, \quad (1)$$

which is the starting point for the calculation.[10,22,23]

LILITA uses different approximations for evaluating the level densities $\rho(\epsilon_\alpha,I_\alpha)$, depending on whether the excitation energy under consideration is in the continuum region or the discrete region. The level densities in the continuum region of the various nuclides were determined from a constant temperature approximation to the Fermi gas formula.[21] The discrete level densities are uniform level densities equal to the average level density for the discrete region.

The information needed by the computer code LILITA includes the A and Z of the projectile and target and the laboratory energy. Also, the exact masses of the projectile, target, compound nucleus, and every allowed residual nucleus in the N-by-Z evaporation matrix are needed for the calculation. These values were obtained from Refs. 24 and 25. The critical angular momentum was calculated using the classical equation

$$J_{\rm crit}=0.219R[\mu(E_{\rm c.m.}-V_c)]^{1/2},$$

where

$$R=1.5(A_t^{1/3}+A_p^{1/3})$$

and

$$V_c=1.44Z_tA_p/R,$$

and $E_{\rm c.m.}$ is the center of mass energy. V_c is the Coulomb barrier and R is the grazing distance. The actual $J_{\rm crit}$ values used are listed in Table I. In addition, the calculation requires that pairing energies, threshold energies, and cutoff energies be supplied for each evaporation residue in the N-by-Z evaporation matrix. The pairing energies were obtained from Ref. 21 and the threshold and cutoff energies were obtained from the separation energies listed in Ref. 25. The ground state spins and discrete level densities of the residual nuclei in the N-by-Z evaporation matrix were taken from the Nuclear Data Sheets. The discrete densities were chosen as uniform level densities calculated from the number of known levels up to the cutoff energy.

In the discrete region LILITA uses the Fermi parametrization

$$T_{l\alpha}=\frac{C_\alpha}{1+e^{(B_l-\epsilon)}/\Delta\epsilon^*_\alpha B_l}$$

to calculate the transmission coefficients. ϵ is the

TABLE I. The critical angular momenta used in the LILITA calculations. The beam was ^{28}Si.

^{27}Al target		^{28}Si target		^{54}Fe target		^{56}Fe target	
E (MeV)	J_{crit}	E (MeV)	J_{crit}	E (MeV)	J_{crit}	E (MeV)	J_{crit}
62.9	11	62.6	5	79.6	10.5	78.3	11
70.0	18	69.7	15	84.6	20.5	83.3	21
75.0	21	74.8	19	89.6	27.0	88.3	28
79.1	24	78.8	22	94.6	32.0	93.4	33
		82.8	25	98.6	35.5	97.4	37
		87.9	27				

center of mass energy. C_α and Δ_{C_α} are parameters determined from optical model transmission coefficients using standard techniques. α takes on the values n, p, or α (neutron, proton, or alpha particle, respectively), for the type particle evaporation allowed. The barrier energy (centrifugal plus Coulomb) is

$$B=\frac{Z_1Z_2e^2}{R_c}+\frac{h^2}{2\mu_c R_c^{\,2}}(l+1/2)^2$$

and μ_c is the reduced mass.[10] These transmission coefficients did not differ greatly from those used by ALICE.

Continuum level densities were calculated using a Fermi gas level density including a pairing energy correction.[21] Initially the level density parameter a was chosen equal to 7.5, then it was varied by up to ten percent to obtain the best possible fit to the data. This technique was used at both the lowest and highest energies for which data were taken, then an average for each value of a (the level density parameter) was obtained. These average values were then used for the LILITA calculations at all energies. Much larger variations of the level density parameters were tried, but they did not improve the overall quality of agreement. The fits for some residual nuclei became better, while those for others became worse.

In addition to the above parameters a transmission coefficient cutoff parameter[23] was set equal to 10^{-5} and the moment of inertia $\mathscr{I}$ was set equal to one half the rigid body moment of inertia $\mathscr{I}_{rig}$. Changing the transmission cutoff parameter from 10^{-5} to 10^{-7}, the moment of inertia from $\frac{1}{2}\mathscr{I}_{rig}$ to $\mathscr{I}_{rig}$, and the critical angular momentum by a few units of angular momenta had a net effect of about 10% on the calculations. This is believed insignificant since errors in the data are 10 to 20%.

IV. RESULTS

The results of the comparison of the experimental evaporation residue cross sections with those obtained from the evaporation model calculations ALICE and LILITA are presented below. It should be noted that the normalization of the data to the calculations in all cases was obtained by summing the cross sections for all experimental reaction products and setting this sum equal to the same summation for each of the calculations.

A. ^{27}Al+^{28}Si

The experimental relative cross sections for the excitation functions of the reaction products produced in the ^{27}Al+^{28}Si reaction are given in Table II. Figure 1 shows the data, as well as the results of the ALICE calculation, for the excitation functions of the reaction products produced in the ^{27}Al+^{28}Si reaction. As indicated in the figure, the shapes of the three-particle evaporation ^{49}V($\alpha 2p$), ^{49}Cr(αpn), ^{52}Mn($2pn$), and ^{52}Cr($3p$) excitation functions are fairly well reproduced by this calculation. However, the calculation underpredicts the experimental results by a factor of 2 for ^{49}V and ^{49}Cr, while it overpredicts the experimental results by about a factor of 2 for ^{52}Mn. In the case of four-particle evaporations ^{51}Cr($3pn$) and ^{51}Mn($2p2n$), the ALICE calculation peaks at too high an energy, although the magnitude of the calculation is approximately correct. ALICE underpredicts ^{50}Cr(αp), the two particle evaporation, by a factor of 4 and is peaking at much too low

TABLE II. Experimental relative reaction product cross sections produced in the reaction ^{27}Al+^{28}Si.

	E_L (MeV)			
Product	62.9	70.0	75.0	79.1
^{52}Mn($2pn$)	76	100	107	92
^{51}Mn($2p2n$)	2.3	5.8	9.8	16
^{52}Cr($3p$)	48	49	44	41
^{51}Cr($3pn$)	5.9	33	70	114
^{50}Cr(αp)	33	44	52	58
^{49}Cr(αpn)	5.6	41	65	86
^{49}V($\alpha 2p$)	45	100	134	201

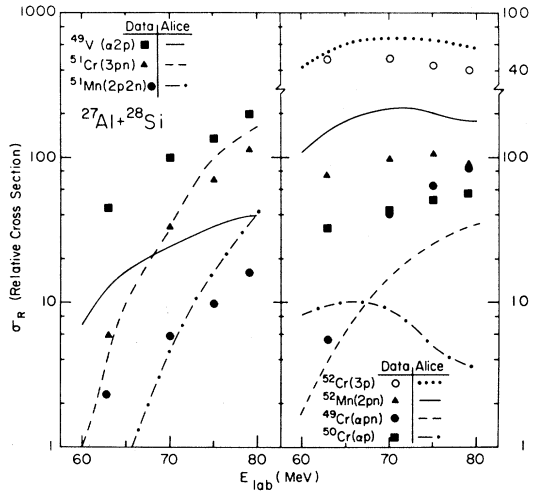

FIG. 1. Comparison of the evaporation model calculation ALICE to experimental excitation functions for the products of the reaction ^{27}Al+^{28}Si.

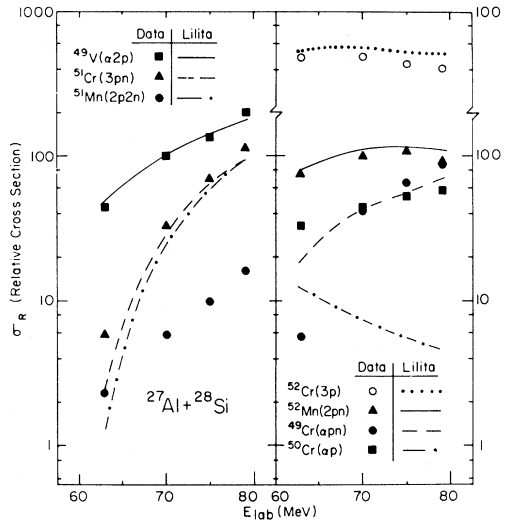

FIG. 2. Comparison of the LILITA evaporation model calculation to the experimental excitation functions for the products of the reaction ^{27}Al+^{28}Si.

an energy—at least 15 MeV lower than the data.

Figure 2 displays the LILITA calculations and experimental data for the excitation functions of the reaction products produced in the ^{27}Al+^{28}Si reaction. LILITA calculations for the reaction products resulting from the evaporation of three particles, ^{49}V($\alpha 2p$), ^{52}Cr($3p$), ^{52}Mn($2pn$), and ^{49}Cr(αpn), reproduce the data extremely well. That is, both the magnitude and shape of the calculated excitation functions agree with the data very well for three-particle evaporations. The shapes of the excitation functions for four-particle evaporation [namely, ^{51}Cr($3pn$) and ^{51}Mn($2p2n$)] are well predicted by this calculation. The ^{51}Cr($3pn$) magnitude also agrees with the calculation; however, the calculation overpredicts the magnitude of ^{51}Mn($2p2n$) by about a factor of 4. The LILITA calculation for the two-particle evaporation ^{50}Cr(αp) also poorly predicts the shape and magnitude of the cross section.

Both calculations ALICE and LILITA are deficient in predicting both the magnitudes and shapes of the excitation function for the reaction product ^{50}Cr(αp). Both calculations are sensitive to the level density parameters a which are poorly known in this mass and energy region.

B. ^{28}Si+^{28}Si

Experimental excitation functions for the relative cross sections of the reaction products produced with the reaction ^{28}Si+^{28}Si are given in Table III. A plot of the calculated excitation functions from ALICE and the data for the reaction products produced in the reaction ^{28}Si+^{28}Si are shown in Fig. 3. As shown in this figure the only reaction products that are well predicted by ALICE in both shape and magnitude are ^{52}Cr($4p$) and ^{53}Fe($2pn$). Other three- and four-particle evaporations are not as well reproduced. The shapes of the excitation functions for

TABLE III. Experimental relative reaction product cross sections produced in the reaction ^{28}Si+^{28}Si.

	E_L (MeV)					
Product	62.6	69.7	74.8	78.8	82.8	87.9
^{54}Fe($2p$)	18	29	27	23	16	11
^{53}Fe($2pn$)	10	40	70	70	58	44
^{53}Mn($3p$)	22	58	100	114	110	97
^{52}Mn($3pn$)		2	7	12	22	30
^{51}Mn(αp)	1	3	5	6	5	5
^{52}Cr($4p$)		9	17	25	30	35
^{50}Cr($\alpha 2p$)	11	40	67	98	120	140

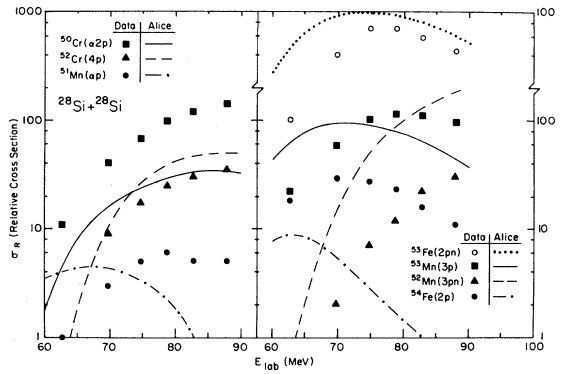

FIG. 3. ALICE calculations compared with the experimental excitation functions for the products of the reaction ^{28}Si+^{28}Si.

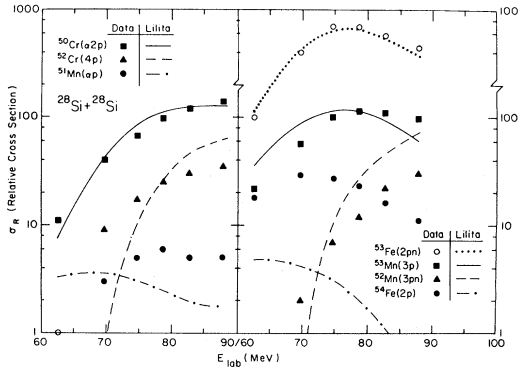

FIG. 4. LILITA evaporation model calculations compared with excitation functions of products of the reaction ^{28}Si+^{28}Si.

the two-particle evaporations ^{54}Fe($2p$) and ^{51}Mn(αp), as well as the magnitudes for these products are poorly predicted by ALICE.

A graph of the excitation functions of the reaction products from the ^{28}Si+^{28}Si reaction along with the LILITA calculations for this reaction is shown in Fig. 4. Excitation functions resulting from the evaporation of three particles, ^{50}Cr($\alpha 2p$), ^{53}Fe($2pn$), and ^{53}Mn($3p$), are well reproduced in both shape and magnitude by LILITA, although ^{53}Mn($3p$) peaks about 5 MeV too low. Magnitudes of the four-particle evaporations ^{52}Cr($4p$) and ^{52}Mn($3pn$) are well predicted by the calculation, but the calculation peaks at too high an energy in both cases. Again, the two-particle evaporations are underpredicted, in the case of ^{54}Fe by a factor of 7. The calculations for both ^{51}Mn(αp) and ^{54}Fe($2p$) peak at too low an energy.

Comparing Figs. 3 and 4, i.e., ALICE and LILITA, for the reactions ^{28}Si+^{28}Si, one sees that LILITA does a better job of fitting the data than ALICE. Both LILITA and ALICE are deficient in reproducing the two-particle-evaporation reaction products, indicating that some other effect is important that is being ignored in the calculation for two-particle evaporation products.

C. ^{54}Fe+^{28}Si

The calculations discussed above have been extended into the mass $A \sim 80$ region using the ^{54}Fe+^{28}Si reaction. Table IV gives the results of the experimental data for the reaction products measured in this reaction. One of the shortcomings of using this reaction is that the ground state transition for ^{79}Sr is unknown, so the relative cross section for this reaction product could not be measured. Also ^{79}Sr is predicted to be one of the strongest reaction products in both calculations. This does have an effect on the overall normalization, but is not expected to affect the relative cross sections to a great extent.

ALICE calculations for the excitation functions of the reaction products measured in the ^{54}Fe+^{28}Si reaction are shown along with the data in Fig. 5. The calculation agrees in both magnitude and shape with the experimental cross sections of the four-particle evaporation products ^{78}Rb($3pn$) and ^{78}Kr($4p$), although the calculation for ^{78}Kr($4p$) peaks at too low an energy. ^{79}Rb($3p$) and ^{76}Kr($\alpha 2p$), resulting from the evaporation of three particles, are well predicted in magnitude by the calculation. However, the shapes of the calculated excitation functions for these two products are incorrect. They peak at too low an energy. In the case of ^{79}Rb($3p$) the calcula-

TABLE IV. Experimental relative reaction product cross sections produced in the reaction ^{54}Fe+^{28}Si.

Product	E_L (MeV) 79.6	84.6	89.6	94.6	98.6
^{80}Sr($2p$)	28.2	39.7	41.6	40.6	33.4
^{79}Rb($3p$)	32.4	67.1	100.0	143.2	158.9
^{78}Rb($3pn$)		9.2	39.8	86.3	152.3
^{78}Kr($4p$)		6.5	22.9	64.0	106.5
^{76}Kr($\alpha 2p$)	7.7	24.6	53.8	105.9	142.3

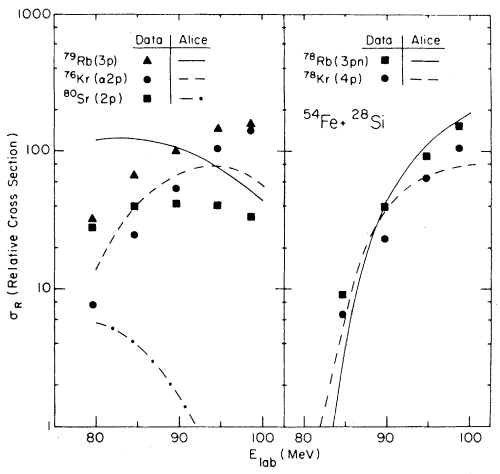

FIG. 5. Experimental excitation functions for the reaction ^{54}Fe+^{28}Si, compared with the evaporation model calculation ALICE.

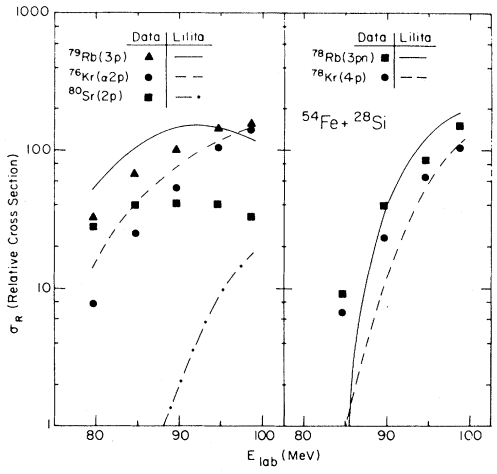

FIG. 6. Comparison of the evaporation model calculation LILITA to the excitation functions of the products of the reaction ^{54}Fe+^{28}Si.

tion is peaking at a laboratory energy 15 MeV lower than the data. Again, as was the case in the mass $A \sim 50$ region, both the shape and magnitude of the two-particle evaporation are poorly reproduced.

LILITA calculations for the excitation functions of the reaction products from the ^{54}Fe+^{28}Si reaction along with the data are shown in Fig. 6. The LILITA calculation agrees well with the data for the evaporation of four particles. Both the shapes and magnitudes of the excitation functions of ^{78}Kr($4p$) and ^{78}Rb($3pn$) are well reproduced by this calculation. The three-particle evaporations ^{76}Kr($\alpha 2p$) and ^{79}Rb($3p$) are well predicted in magnitude by this calculation. The ^{76}Kr($\alpha 2p$) shape is also well reproduced, but the ^{79}Rb($3p$) calculation peaks at 5 to 10 MeV below where the data peaks. For ^{80}Sr($2p$), the two-particle evaporation, both the shape and magnitude of the excitation function are poorly predicted by LILITA. However, ALICE predicts this product to fall off rapidly with energy, and LILITA has it increasing rapidly with energy. In both cases two-particle evaporations are poorly predicted.

D. ^{56}Fe+^{28}Si

The reaction ^{56}Fe+^{28}Si was also used to compare the evaporation model calculations ALICE and LILITA in the mass $A \sim 80$ region. Table V gives the results of the experimentally measured excitation functions for this reaction.

None of the reaction products produced in the ^{56}Fe+^{28}Si reaction are predicted correctly by ALICE. In all cases the shapes of the calculated excitation functions are incorrect (see Fig. 7). ALICE for the three-particle evaporations ^{81}Sr($2pn$), ^{81}Rb($3p$), and ^{78}Kr($\alpha 2p$), predicts the excitation functions to peak at a much lower energy than the data peaks. However, the magnitudes of the calculated excitation functions for these products are approximately correct. The magnitude of ^{80}Kr($4p$) is reasonably well predicted by ALICE, but the calculation also

TABLE V. Experimental relative reaction product cross sections produced in the reaction ^{56}Fe+^{28}Si.

Product	E_L (MeV) 78.3	83.3	88.3	93.4	97.4
^{82}Sr($2p$)	31.3	47.1	57.4	55.5	42.6
^{81}Sr($2pn$)	44.8	81.0	100.0	117.6	129.3
^{80}Sr($2p2n$)			6.0	12.6	19.2
^{81}Rb($3p$)	17.0	29.6	40.9	47.9	50.8
^{79}Rb(αp)	5.3	14.5	20.1	21.0	19.9
^{80}Kr($4p$)		5.1	12.7	21.1	30.0
^{78}Kr($\alpha 2p$)	11.9	39.0	66.5	103.6	134.8

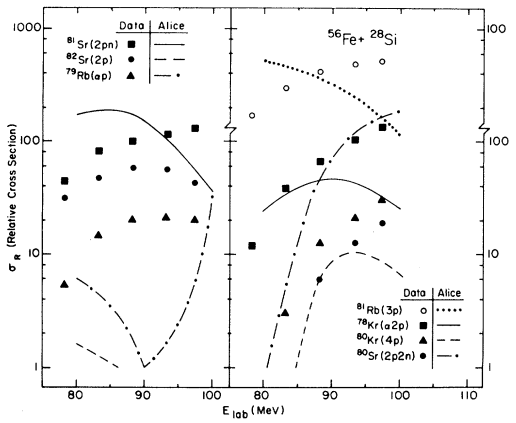

FIG. 7. ALICE evaporation model calculations compared with the experimental excitation functions of products of the reaction $^{56}Fe+^{28}Si$.

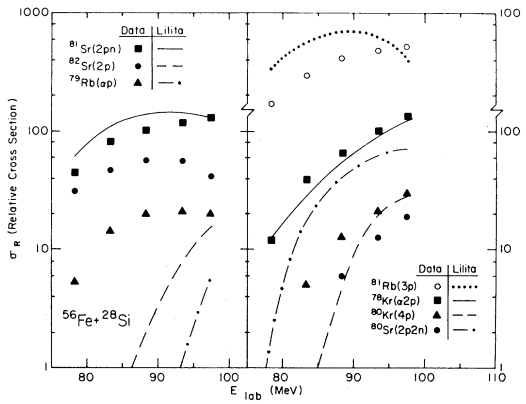

FIG. 8. Comparison of the evaporation model calculation LILITA to the experimental excitation functions of the products of the reaction $^{56}Fe+^{28}Si$.

peaks at too low an energy. The shape of the calculated excitation function for the evaporation product $^{80}Sr(2p2n)$ is incorrect. In this case ALICE peaks at too high an energy, and it overpredicts the data by about a factor of 9. $^{82}Sr(2p)$ and $^{79}Rb(\alpha p)$, the two-particle evaporation products, are poorly reproduced by ALICE. Both the shapes and the magnitudes of the calculated excitation functions do not agree with the data. The unusual shape of the calculated $^{79}Rb(\alpha p)$ excitation function can possibly be explained by the fact that part is due to the two-particle evaporation αp and the balance is due to the five-particle evaporation $3p2n$.

Results of the LILITA calculation for the reaction $^{56}Fe+^{28}Si$ are shown in Fig. 8. LILITA predicts both the shapes and magnitudes of the three-particle evaporation products $^{81}Sr(2pn)$, $^{78}Kr(\alpha 2p)$, and $^{81}Rb(3p)$, although the $^{81}Rb(3p)$ calculation peaks about 7 MeV lower than the data. The shape of the calculated excitation functions for the four-particle evaporations, namely, $^{80}Kr(4p)$ and $^{80}Sr(2p2n)$, also agrees with the data. However, $^{80}Sr(2p2n)$ is overpredicted by about a factor of 6. The calculated excitation functions for $^{79}Rb(\alpha p)$ and $^{82}Sr(2p)$ do not reproduce the data to any extent. Both calculations peak at much too high an energy, and the magnitudes are underpredicted by a factor of about 10 to 20.

Comparing ALICE and LILITA calculations for the reaction $^{56}Fe+^{28}Si$ (Figs. 7 and 8), one sees that LILITA is superior to ALICE in most cases, although the two-particle evaporations are poorly reproduced by both calculations.

V. CONCLUSIONS

In the discussion above, the compound nuclear evaporation model calculations, ALICE (Ref. 9) and LILITA,[10] were compared with the experimental reaction product relative cross sections in the mass $A\sim 50$ region using the reactions $^{27}Al+^{28}Ai$ and $^{28}Si+^{28}Si$. This study was also carried out in the mass $A\sim 80$ region using the reactions $^{54}Fe+^{28}Si$ and $^{56}Fe+^{28}Si$. Several conclusions can be drawn.

(1) The results of this investigation indicate that LILITA generally reproduces the data better than ALICE. Since LILITA includes conservation of angular momentum in the exit channel and ALICE does not, these results suggest that angular momentum effects are important in both mass regions. This has previously been shown to be true for heavy-ion reactions.

(2) ALICE reproduces the data better in the mass $A\sim 50$ region than in the mass $A\sim 80$ region, while LILITA does an equivalent job in both mass regions. This suggests that angular momentum effects may be more important in the mass $A\sim 80$ region.

(3) Some deficiencies in the calculations may be explained by the uncertainty in the continuum level-density parameters a. The evaporation model calculations are very sensitive to these level-density parameters; $a\simeq A/7.5$ for each residual nucleus. These parameters are not very well known in either mass region and were adjusted somewhat in the present calculations.

(4) Finally, the two-particle evaporations are badly underpredicted by both calculations in both mass regions. One possible explanation is that the two-particle reaction product cross sections may be partially due to some mechanism other than the compound nuclear reaction. An investigation into this phenomenon is continuing at Florida State University.

Other investigations[26] have also shown the importance of a proper treatment of angular momentum in the statistical decay process. A number of com-

parisons have been made between experimental evaporation residue measurements and the results of LILITA calculations for compound nuclei around mass 30.[22,23,27,28] Reasonably good agreement was seen between the calculated and predicted distribution of evaporation residue strength for these light systems. Another code which treats angular momentum in statistical multiparticle decay is CASCADE.[29] Several comparisons of the results of this code with experimental data for compound nuclei in the mass 30 to 50 range have reported reasonably good agreement.[29–31] CASCADE has been reported,[30] however, to badly underpredict the cross section of nuclei produced when only one particle is emitted from the compound nucleus. It is possible that this failure is related to the underprediction of two-nucleon emission observed here.

ACKNOWLEDGMENTS

The authors wish to thank Bob Leonard for the preparation of the evaporated targets. Also, we wish to thank L. C. Dennis for the many discussions on the computer code LILITA and compound nuclear calculations in general. These discussions were invaluable to the completion of this work. This work was supported in part by the National Science Foundation.

---

*Present address: Bell Telephone Laboratories, Holmdel, NJ 07733.

†Present address: Department of Computer and Information Science, New Jersey Institute of Technology, Newark, NJ 07102.

[1]J. S. Clements, L. R. Medsker, L. H. Fry, Jr., and L. V. Theisen, Phys. Rev. C 21, 1285 (1980).

[2]H. Gauvin, D. Guerreau, Y. LeBeyec, M. Lefort, F. Plasil, and X. Tarrago, Phys. Lett. 58B, 163 (1975).

[3]M. Beckerman and M. Blann, Phys. Lett. 68B, 31 (1977).

[4]I. Dostrovsky, Z. Fraenkel, and Friedlander, Phys. Rev. 116, 683 (1959).

[5]L. R. Medsker, D. C. Wilson, and L. H. Fry, Jr., Phys. Lett. 74B, 39 (1978).

[6]L. R. Medsker, L. H. Fry, Jr., and D. C. Wilson, Phys. Rev. C 18, 2584 (1978).

[7]L. R. Medsker, L. V. Theisen, L. H. Fry, Jr., and J. S. Clements, Phys. Rev. C 19, 790 (1979).

[8]L. V. Theisen, S. L. Tabor, L. R. Medsker, G. Neuschaefer, L. H. Fry, Jr., and J. S. Clements, Phys. Rev. C 25, 1325 (1982).

[9]M. Blann, Rochester University NSRL Report No. C00-3493-34, 1977 (unpublished).

[10]J. Gomez del Campo and R. G. Stokstad, Oak Ridge National Laboratory report, 1977 (unpublished).

[11]V. F. Weisskopf, Phys. Rev. 52, 295 (1937).

[12]V. F. Weisskopf and D. H. Ewing, Phys. Rev. 57, 472 (1940).

[13]W. Hauser and H. Feshback, Phys. Rev. 87, 366 (1952).

[14]K. R. Chapman, Nucl. Instrum. Methods 124, 229 (1975).

[15]Mixed radionuclide standard (4215E) from the National Bureau of Standards.

[16]The code PEAKFIT courtesy of P. S. Singh, Indiana University Cyclotron Facility. Modified by R. V. LeClaire for interactive use at Florida State University.

[17]J. O. Newton, F. S. Stephens, R. M. Diamond, K. Kotojima, and E. Matthais, Nucl. Phys. A95, 357 (1967).

[18]P. Taras and B. Haas, Nucl Instrum. Methods 123, 73 (1975).

[19]R. M. Diamond, E. Matthais, J. O. Newton, and F. S. Stephens, Phys. Rev. Lett. 16, 1205 (1966).

[20]H. A. Bethe, Rev. Mod. Phys. 9, 161 (1931).

[21]A. Gilbert and A. G. W. Cameron, Can. J. Phys. 43, 1446 (1965).

[22]J. Gomez del Campo, R. G. Stokstad, J. A. Biggerstaff, R. A. Dayras, A. H. Snell, and P. H. Stelson, Phys. Rev. C 19, 2170 (1979).

[23]J. J. Kolata, R. M. Freeman, F. Haas, B. Hausch, and A. Gallmann, Phys. Rev. C 19, 408 (1979).

[24]A. H. Wapstra and K. Box, At. Data Nucl. Data Tables 17, 474 (1976).

[25]A. H. Wapstra and K. Bos, At. Data Nucl. Data Tables 19, 177 (1977).

[26]M. Beckerman and M. Blann, Phys. Lett. 68B, 31 (1977); M. Blann, Phys. Rev. 157, 860 (1967).

[27]R. G. Stokstad, J. Gomez del Campo, J. A. Biggerstaff, A. H. Snell, and P. H. Stelson, Phys. Rev. Lett. 36, 1529 (1976).

[28]M. E. Ortiz, J. Gomez del Campo, Y. D. Chen, D. E. Di Gregorio, J. L. C. Ford, D. Shapira, R. G. Stokstad, J. P. F. Sellschop, R. L. Parks, and D. Weiser, Phys. Rev. C 25, 1436 (1982).

[29]F. Pühlhofer, Nucl. Phys. A280, 267 (1977).

[30]S. Gary and C. Volant, Phys. Rev. C 25, 1877 (1982).

[31]K. T. Lesko, D. K. Lock, A. Lazzarini, R. Vandenbosch, V. Metag, and H. Doubre, Phys. Rev. C 25, 872 (1982).